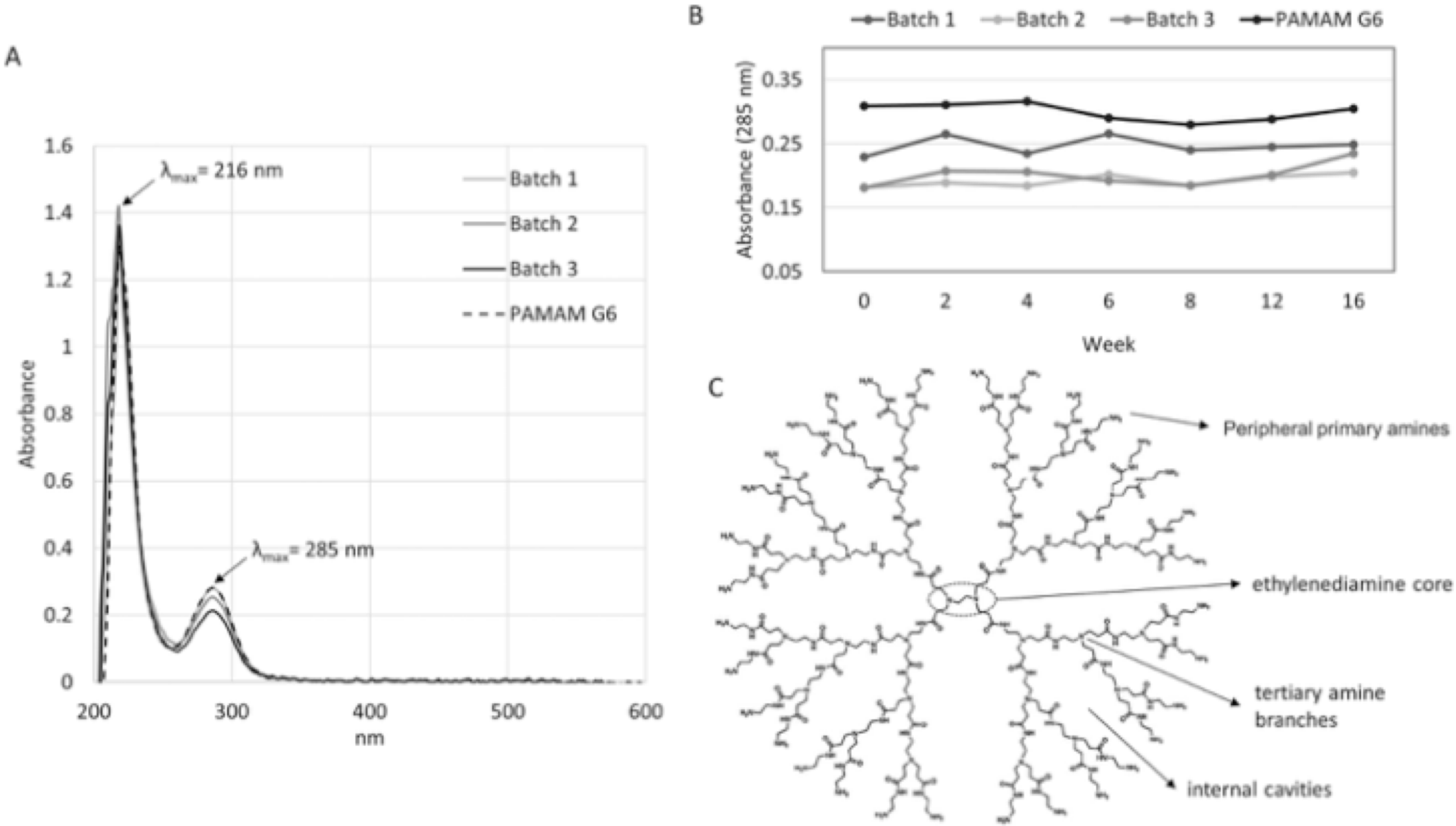

Fig. 1. UV-Vis spectra of OS-PAMAM and PAMAM-G6. (A) Spectrum with characteristic signals of three independent production batches of OS-PAMAM vs PAMAM G6. (B) The signals corresponding to tertiary amides from 280 to 285 nm were taken as a reference value to monitor batches' integrity and control PAMAM-G6 through time until four months at 5 ± 3 °C.(C) Structure of generation 3 (G3) PAMAM dendrimer with amino groups at the periphery.
The ethylenediamine core is circumvented by a dashed line, reproduced from Abbasi et al., 2014 [4].

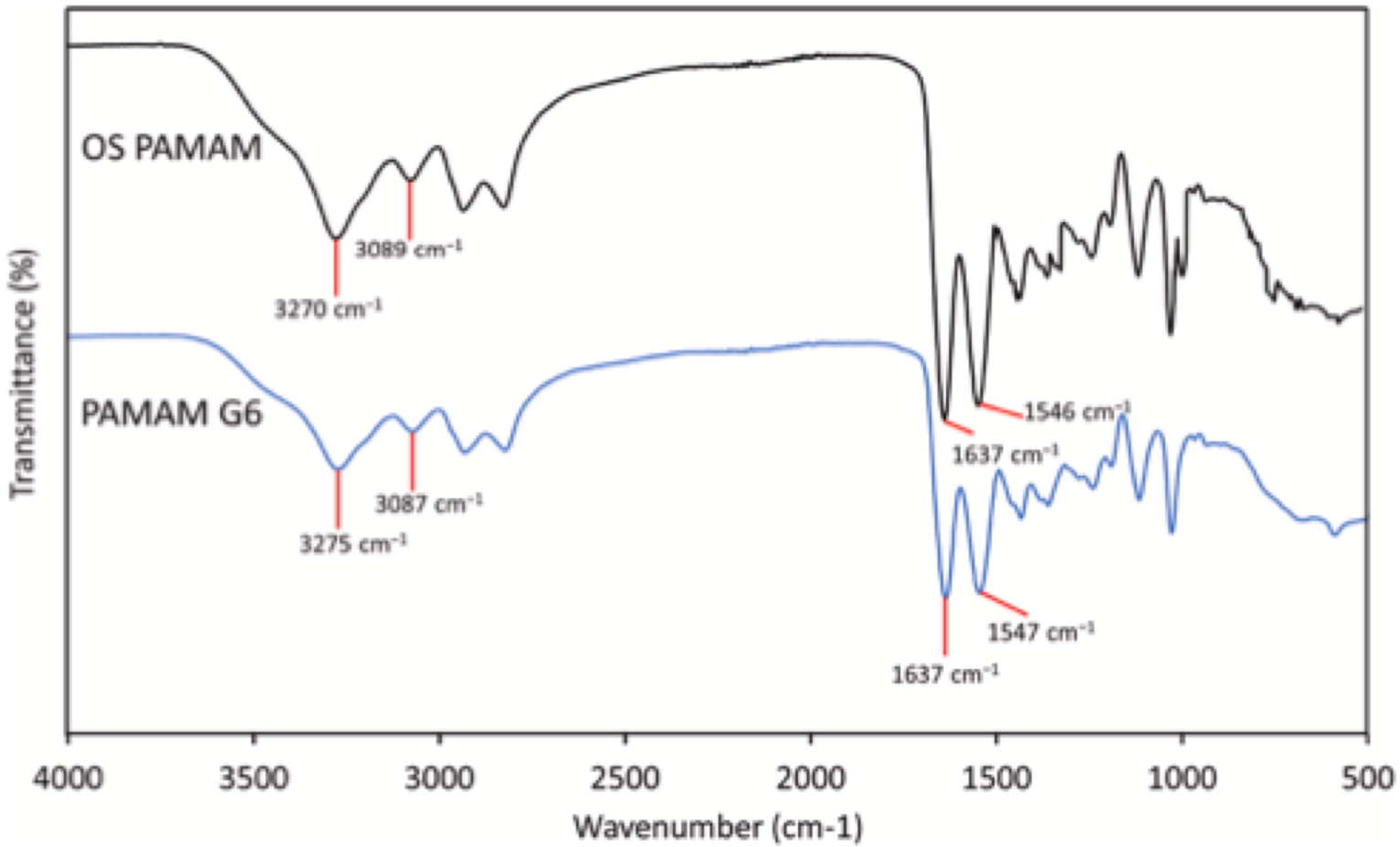

Fig. 2. FT-IR spectra of compared dendrimers. The signals of OS-PAMAM (black) at 3270 cm^{-1} / 1637 cm^{-1} and 3089 cm^{-1} / 1546 cm^{-1} correspond with the signals at 3275 cm^{-1} / 1637 cm^{-1} of primary and 3087 cm^{-1} / 1547 cm^{-1} of secondary amides, respectively, from PAMAM-G6 dendrimers (blue).

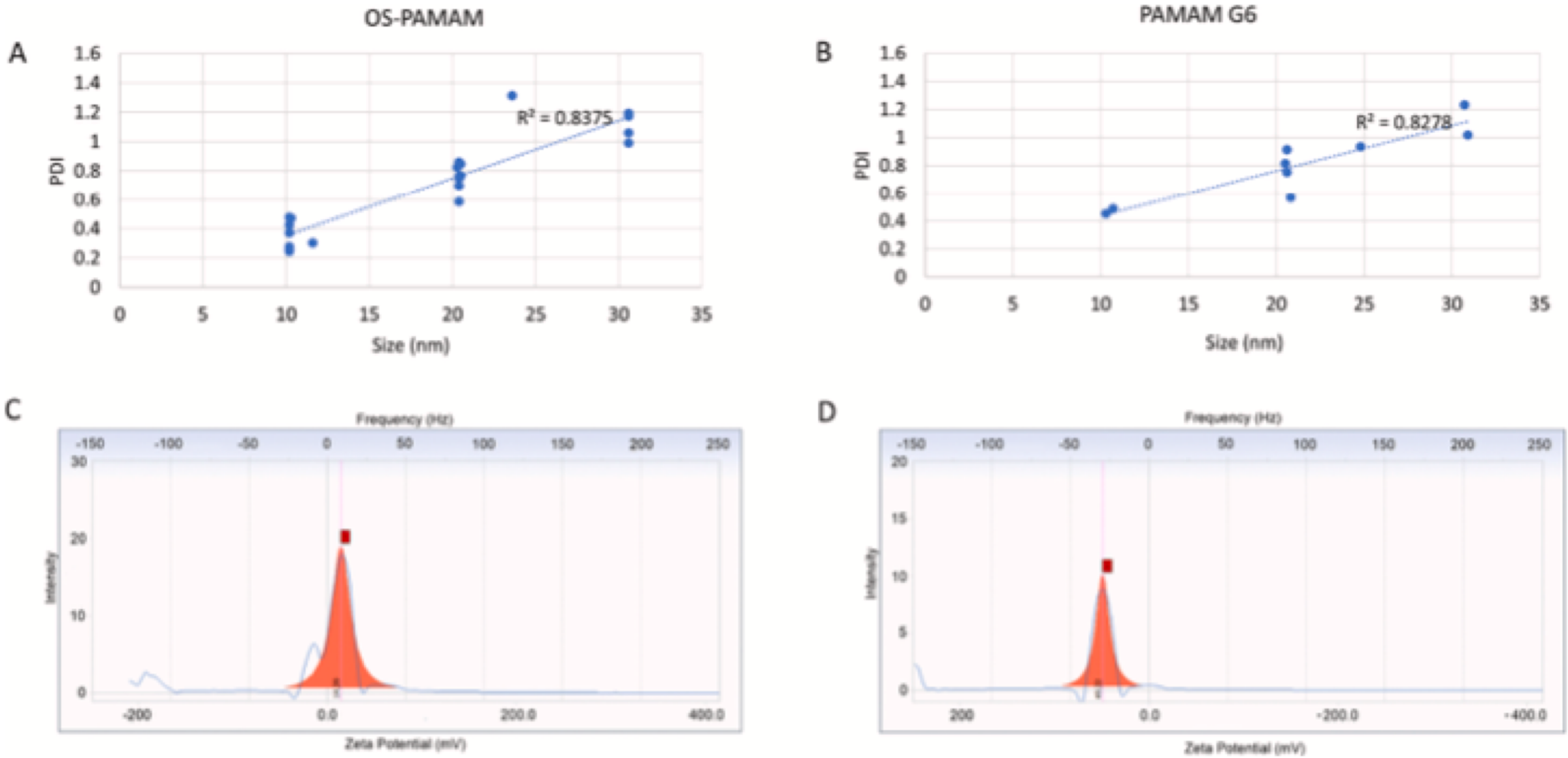

Fig. 3. Size and polydispersity index (PDI) relation and potential zeta profile. The average hydrodynamic sizes as a function of the polydispersity index (PDI) of (A) OS-PAMAM (n = 18) and (B) PAMAM G6 (n = 9) were determined. Representative zeta potential profile of (C) OS-PAMAM and (D) PAMAM G6. All data were obtained under the same analytic method conditions by dynamic light scattering (DLS).

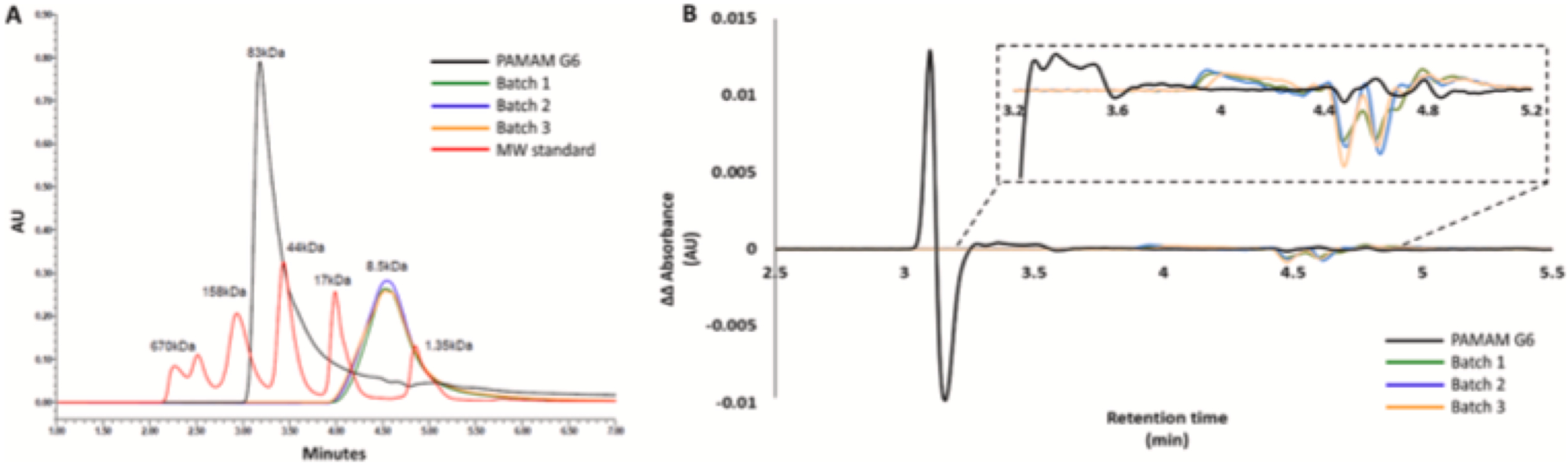

Fig. 4. Molecular weight (MW) between OS-PAMAM batches and PAMAM G6 by SEC. (A) Chromatogram of PAMAM-G6 dendrimer at 215 nm (black line) was compared to three independent batches of OS-PAMAM (green, blue, and orange line) at pH 6.8. MW was determined by linear regression of the maximum value in absorbance units (A.U.) based on the MW standard curve (data not showed). (B) Second derivative analysis of OS-PAMAM batches and PAMAM G6.

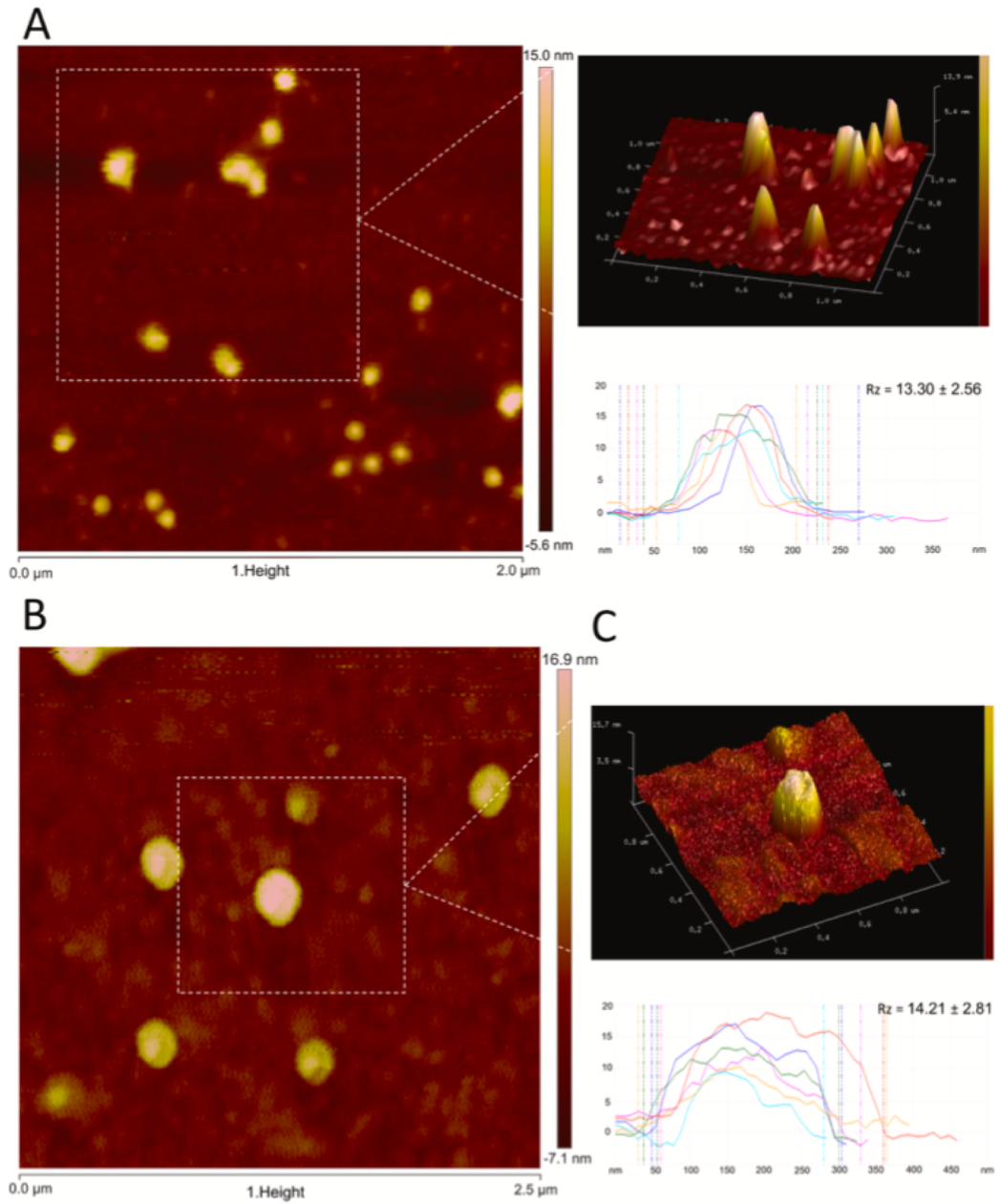

Fig. 5. Size and morphological analysis of dendrimers by AFM. Heightmap of (A) PAMAM-G6 and (B) OS-PAMAM, both average sizes were analyzed through the maximum vertical radius (Rz) of cross-sections (n = 50). (C) The dotted line represents a close-up of the 3D image of the typical shape of OS-PAMAM and PAMAM-G6 dendrimers.

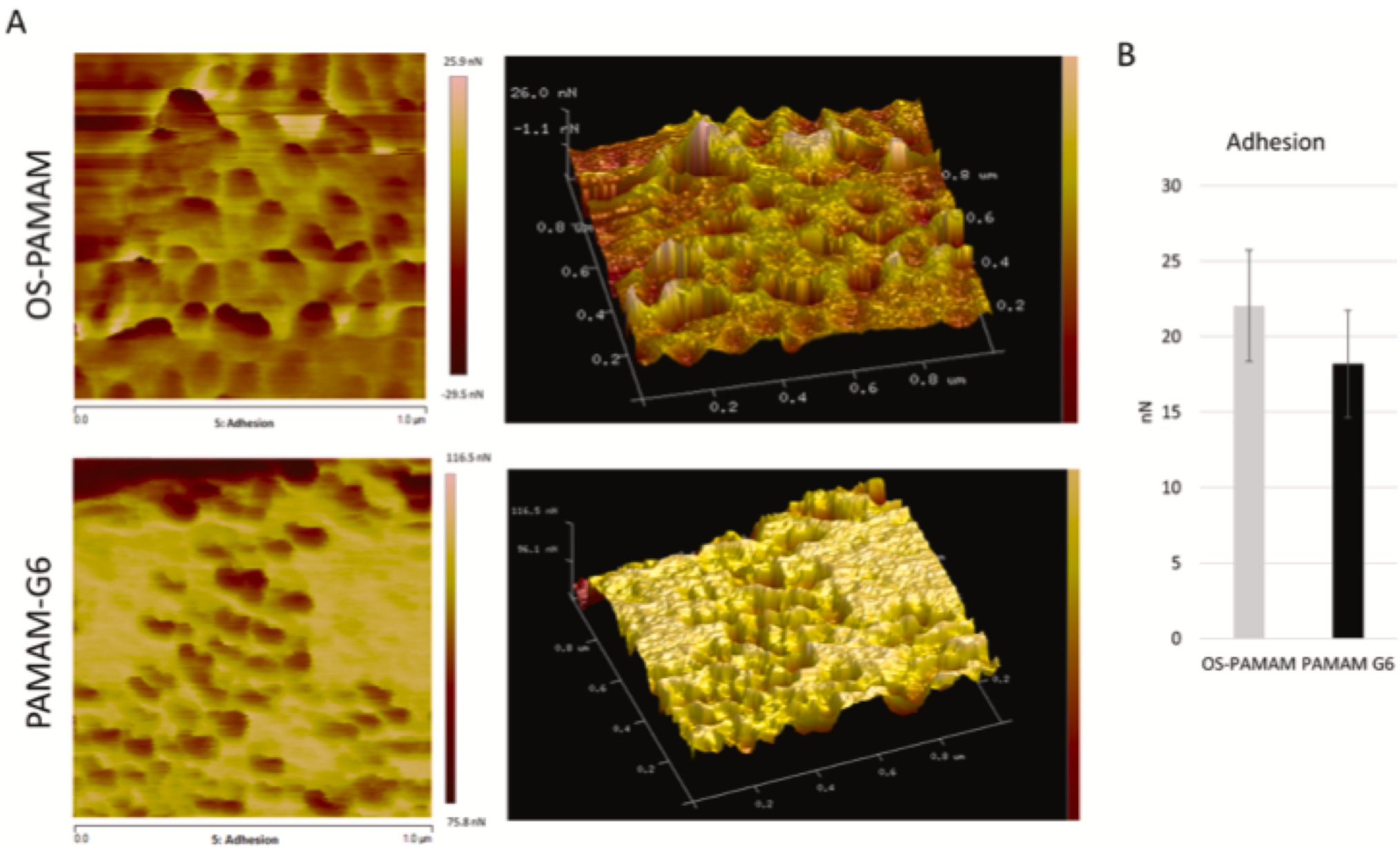

Fig. 6. AFM adhesion force profiles between dendrimers. (A) 2D (left) and 3D (right) topographical imaging of OS-PAMAM and PAMAM-G6 was performed through automatic analysis of curves using NanoScope Analysis Software monitoring force-versus-distance curves. (B) Average adhesion force values (nN) of cross-sections from OS-PAMAM and PAMAM-G6. Data represent mean ± S.D. (n = 50).

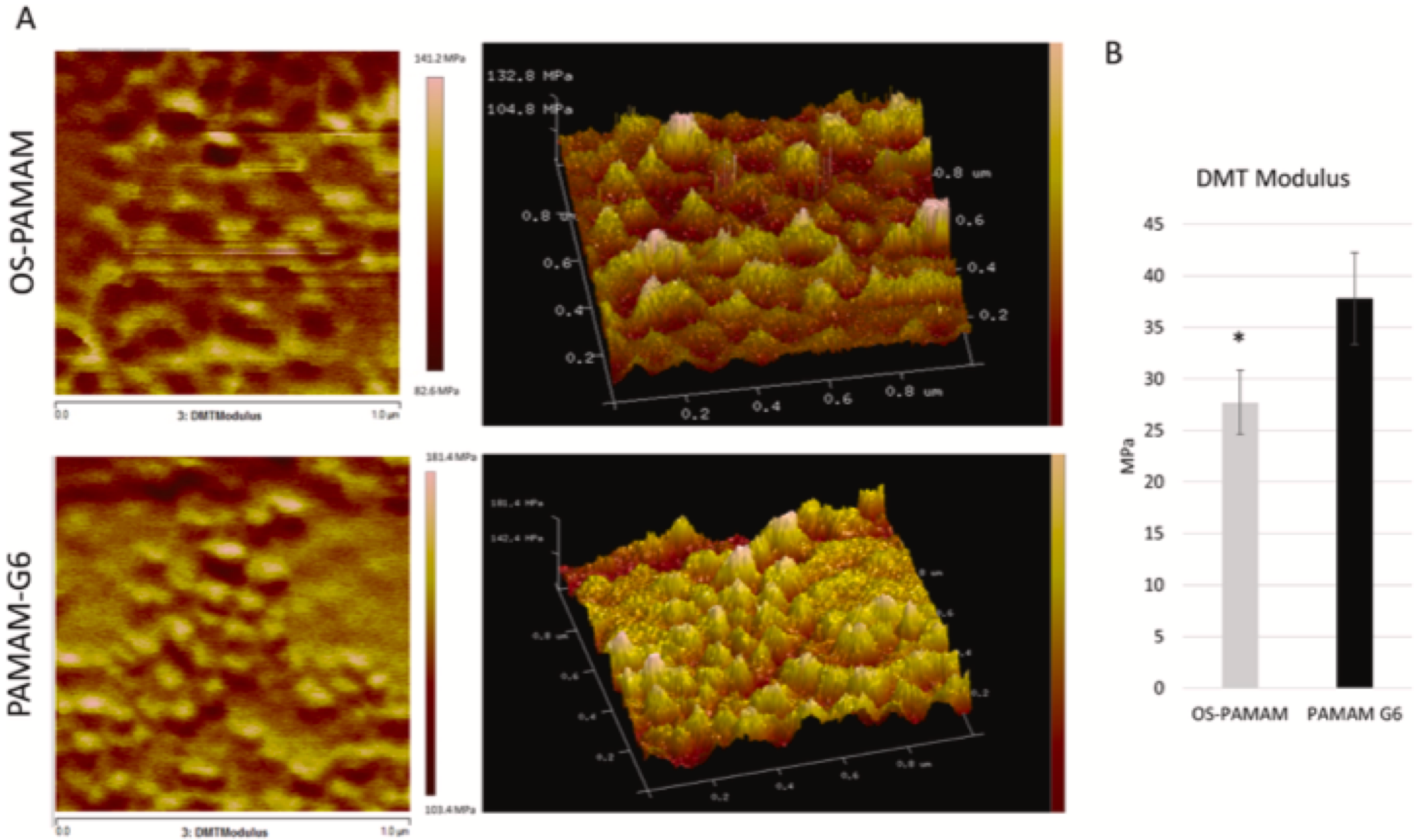

Fig. 7. AFM elasticity modulus differences between OS-PAMAM and PAMAM G6. (A) The elasticity in DMT modulus maps of OS-PAMAM and PAMAM-G6 was performed through automatic analysis of curves using NanoScope Analysis Software comparing hard (slide) and elastic (dendrimers) surfaces. (B) Average elasticity values (MPa) of cross-sections from OS-PAMAM and PAMAM-G6. Data represent mean ± SD (n = 50), * $P < 0.01$ vs OS-PAMAM.

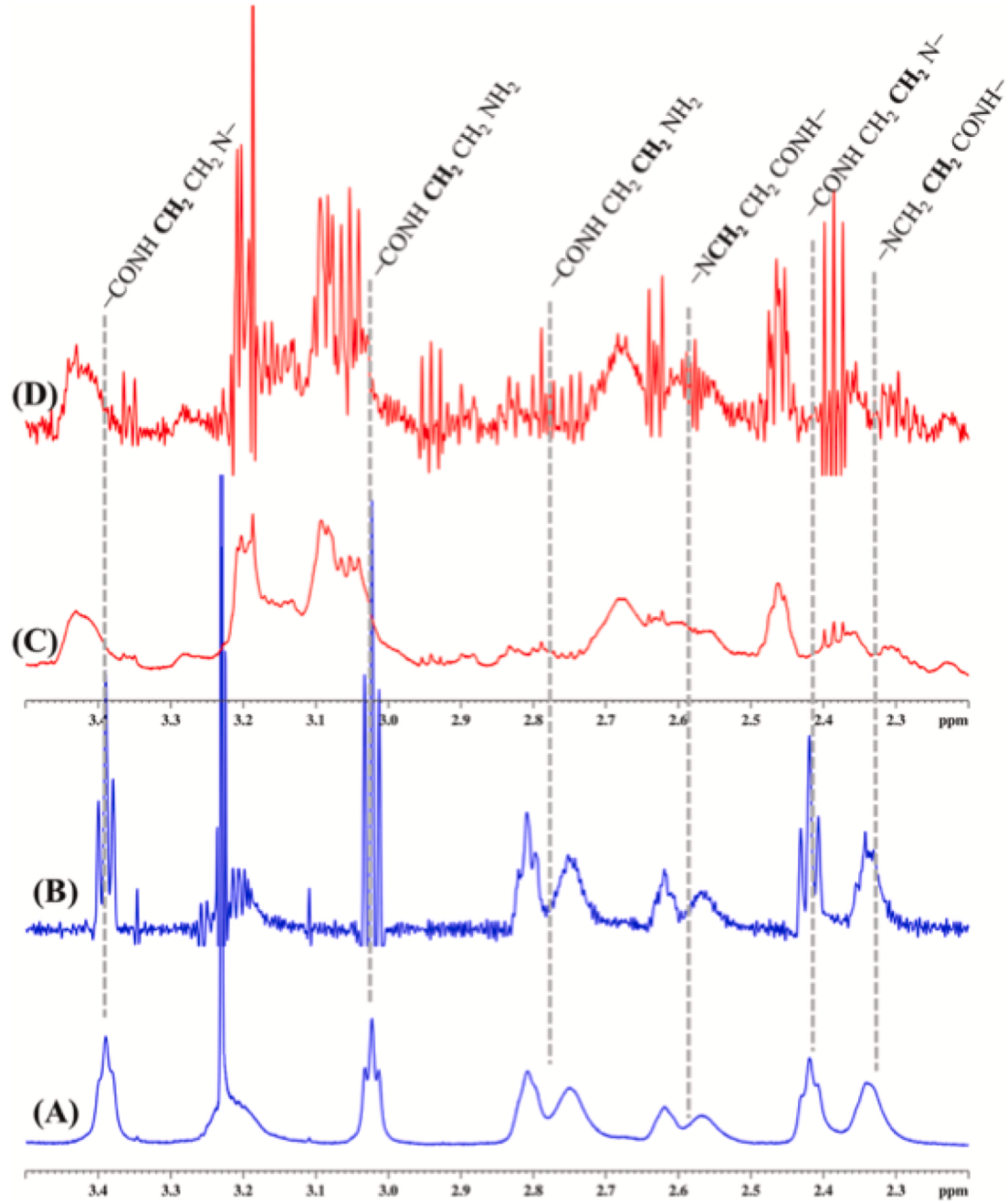

Fig. 8. Standard ^{1}H-one dimensional direct-polarization NMR spectra. Spectra of PAMAM-G6 (blue) and OS-PAMAM (red) with any apodization prior to Fourier Transform (A and C) and proton spectra weighted with a Lorentz to Gauss line sharpening apodization function (B and D) used to reveal sample heterogeneity.

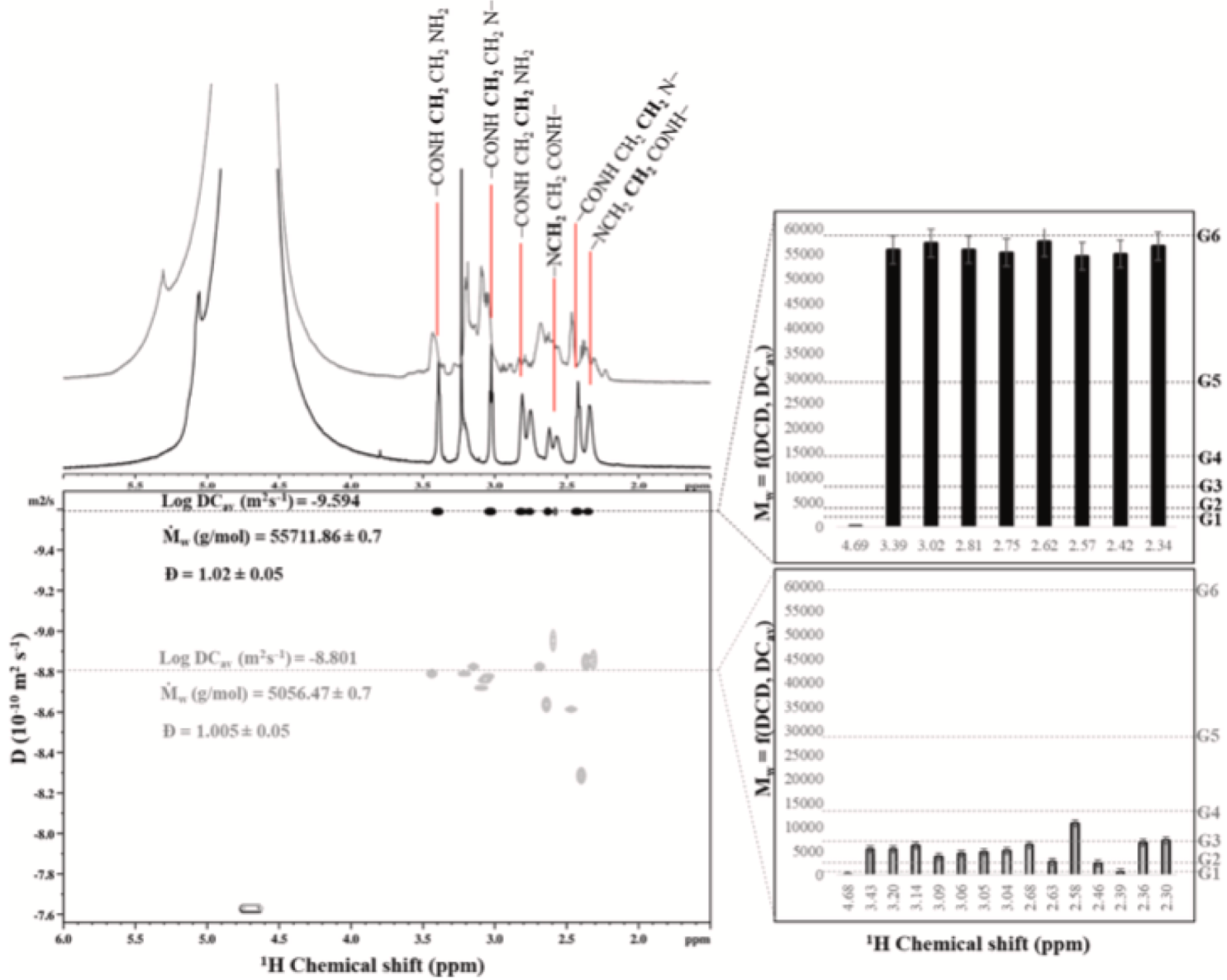

Fig. 9. Solution-state PFG-STE-H2O(presat)-DOSY of PAMAM-G6 and OS-PAMAM. For obtaining average diffusion coefficient distributions (DCD), weighted average molecular weights and polydispersity indexes. (A) PFG-STE-H2O (presat)-DOSY–F2 assigned- NMR spectra of PAMAM batches: Commercial G6 PAMAM (Black) and synthetized OS-PAMAM (gray). Below each logarithmic diffusion coefficient average (Ln DCav, highlighted with a horizontal dotted line) are reported the weight-average molecular weights (Mw) and the polydispersity indexes (PDI) per case. (B) Relative molecular weights [Mw = f(DCD, DCav)] of each chemical-shift assigned resonance obtained from DCD and DCav relationships represented as histograms and expressed in Daltons, are compared with reported molecular weights of PAMAM dendrimers by generation (G1: 1430 Da; G2: 3256 Da; G3: 6909 Da; G4: 14215 Da; G5: 28826 Da and G6: 58048 Da, from http://www.dendritech.com/pamam.html).

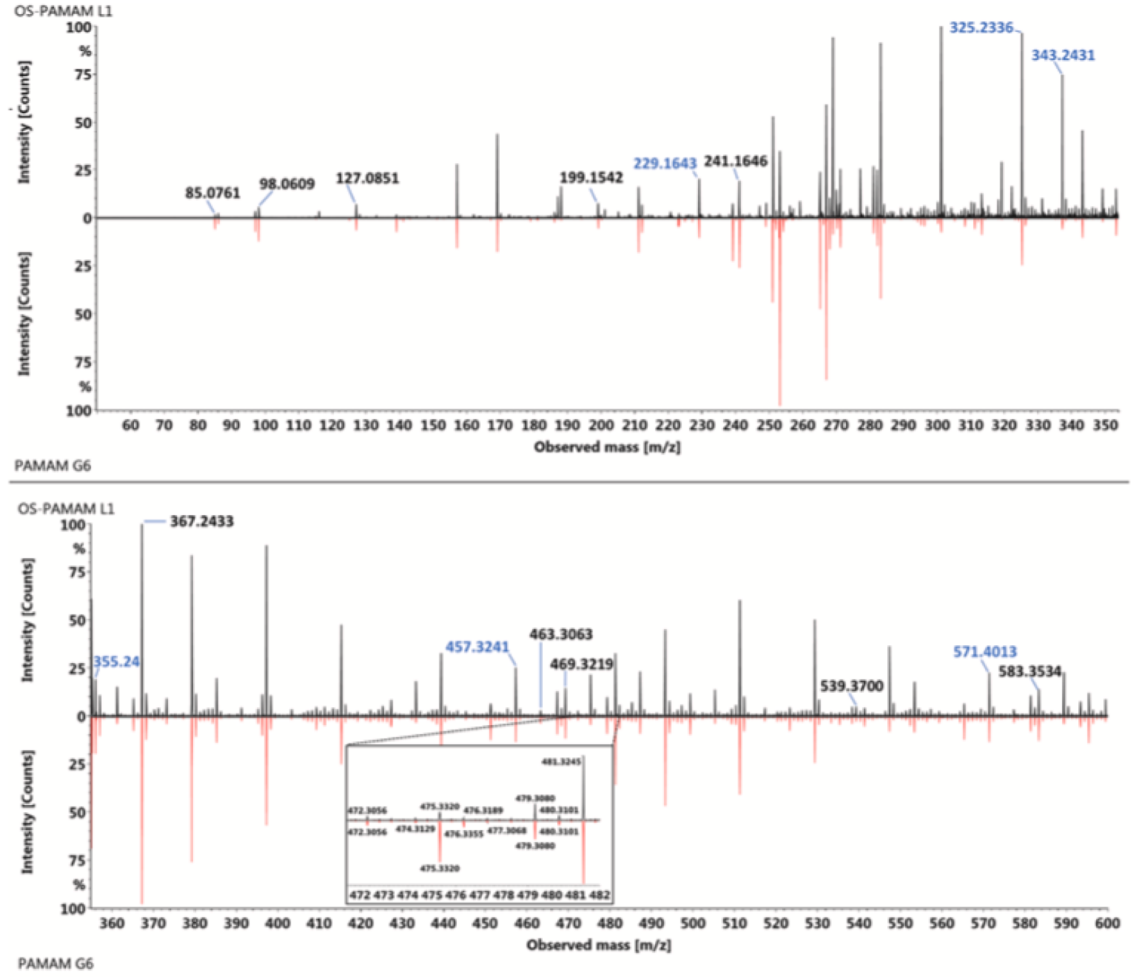

PAMAM precursor ion			
Theoretical mass (m/z)*	Experimental mass (m/z)		PAMAM generation
	OS-PAMAM	PAMAM-G6	
85.0760	85.0761	85.0761	G0, G1, G2 and G3
98.0609	98.0609	98.0710	G1, G2 and G3
127.0866	127.0821	127.1023	G0, G1, G2 and G3
199.1553	199.1542	199.1793	G1, G2 and G3
229.1659	229.1643	229.1912	G1, G2, and G3 fragment
241.1659	241.1646	241.1922	G1, G2 and G3
367.2452	367.2433	367.2457	G3
463.4761	463.3063	463.3008	G2
469.3245	469.3219	469.2778	G3
539.3752	539.3700	539.3700	Precursor ion (major product ion) of G0

Products of PAMAM fragmentation			
Theoretical mass (m/z)*	Experimental mass (m/z)		PAMAM generation
	OS-PAMAM	PAMAM G6	
325.23	325.2336	325.2702	G2
355.24	355.2460	355.2460	G2
343.24	343.2431	343.2855	G3
457.32	457.3241	457.3241	G3
571.40	571.4013	571.4013	G3
583.41	583.3534	583.3534	G3

Fig. 10. LC/ESI-QTOF-MS in high energy spectrum of precursor and fragmentation ions of OS-PAMAM compared with commercial PAMAM-G6. The precursor ions shared between OS-PAMAM and PAMAM-G6 were indicated according to the theoretical values reported for PAMAM G0-G3 and were colored in black. The precursor ions (*m/z*) of OS-PAMAM dendrimers dominated by a common fragmentation pattern based on the retro-Michael mechanism were colored in blue. The table below summarizes the theoretical *m/z* values of the OS-PAMAM and the PAMAM-G6 compared. All OS-PAMAM values present an error of less than 10 ppm concerning the theoretical one. *The theoretical values were obtained from Ulaszewska et al., 2013 [55].